Probabilistic Engineering Mechanics 78 (2024) 103701

Contents lists available at ScienceDirect

Probabilistic Engineering Mechanics

journal homepage: www.elsevier.com/locate/probengmech

A physics-informed neural network enhanced importance sampling (PINN-IS) for data-free reliability analysis

Atin Roy [a,*], Tanmoy Chatterjee [b], Sondipon Adhikari [a]

[a] James Watt School of Engineering, The University of Glasgow, Glasgow, G12 8QQ, United Kingdom
[b] School of Mechanical Engineering Sciences, University of Surrey, Guildford, GU2 7XH, United Kingdom

ARTICLE INFO

Keywords:
Structural reliability
Physics-informed neural network
Data-free
Low failure probability
Importance sampling

ABSTRACT

Reliability analysis of highly sensitive structures is crucial to prevent catastrophic failures and ensure safety. Therefore, these safety-critical systems are to be designed for extremely rare failure events. Accurate statistical quantification of these events associated with a very low probability of occurrence requires millions of evaluations of the limit state function (LSF) involving computationally expensive numerical simulations. Variance reduction techniques like importance sampling (IS) reduce such repetitions to a few thousand. The use of a data-centric metamodel can further cut it down to a few hundred. In data-centric metamodeling approaches, the actual complex numerical analysis is performed at a few points to train the metamodel for approximating the structural response. On the other hand, a physics-informed neural network (PINN) can predict the structural response based on the governing differential equation describing the physics of the problem, without a single evaluation of the complex numerical solver, i.e., data-free. However, the existing PINN models for reliability analysis have been effective only in estimating a large range of failure probabilities (10^{-1}~10^{-3}). To address this issue, the present study develops a PINN-based data-free reliability analysis for low failure probabilities ($<10^{-5}$). In doing so, a two-stage PINN integrated with IS (PINN-IS) is proposed. The first stage is employed to approximate the most probable failure point (MPP) appropriately while the second stage enhances the accuracy of LSF predictions at the IS population centred on the approximated MPP. The effectiveness of the proposed approach is numerically illustrated by three structural reliability analysis examples.

1. Introduction

There are different sources and types of uncertainties in engineering modeling for reliability analyses [1]. Reliability analysis [2] primarily deals with the estimation of failure probabilities based on a performance function or limit state function (LSF), considering the uncertainties of different variables. In structural reliability analysis [3–5], LSF represents a quantity by which the resistance of a structure overcomes the loads acting on it. Therefore, a negative value of LSF represents the failure of the structure. Mathematically, the probability of failure (P_f) is defined as a multi-dimension integral of the joint probability density function (PDF) of random variables over the failure domain. However, the evaluation of the integral is quite difficult due to the irregular shape of the multi-dimensional failure domain. In this regard, various analytical and simulation techniques based approximation are developed. Analytical approaches approximated the LSF around the most probable failure point (MPP) using Taylor series expansion. Depending upon the order of expansion series, analytical approaches are classified as first-order reliability methods (FORM) [6–8] and second-order reliability method (SORM) [9,10]. However, the presence of a disjointed failure domain or multiple MPPs can increase the difficulty in obtaining an unbiased estimate and need special treatment [11]. On the other hand, Monte Carlo simulation (MCS) techniques are based on statistical analysis and random sampling. The brute-force MCS being the most accurate and conceptually straightforward forward is frequently used in reliability analysis. However, the required number of repetitive evaluations of the LSF rises rapidly with the decrease of failure probability and ultimately becomes practically infeasible for estimating low probabilities.

To this end, variance reduction simulation techniques like importance sampling [12–15], subset simulation [16,17], line sampling [18,19], directional simulation [20] etc. are developed to achieve a similar level of accuracy with a considerably reduced number of simulations. Still, several thousand simulations are necessary, and it becomes an

* Corresponding author.
E-mail addresses: Atin.Roy@glasgow.ac.uk (A. Roy), t.chatterjee@surrey.ac.uk (T. Chatterjee), Sondipon.Adhikari@glasgow.ac.uk (S. Adhikari).

https://doi.org/10.1016/j.probengmech.2024.103701
Received 14 May 2024; Received in revised form 27 September 2024; Accepted 12 October 2024
Available online 13 October 2024
0266-8920/

important issue for structural reliability problems that involve computationally expensive numerical techniques to evaluate the LSF. In this regard, the metamodeling technique is an efficient alternative where the LSF is approximated by metamodel trained using the actual structural responses in a limited number of carefully selected data points. Application of polynomial response surface [21,22], Kriging [23,24], artificial neural networks [25,26], radial basis function [27], support vector regression [28–30], sparse Bayesian regression [31,32], polynomial chaos expansion [33,34] etc. can be noted in structural reliability analysis.

Physics-informed neural networks (PINN) recently developed by Raissi et al. [35] is a special type of metamodel that does not require any labelled data for approximating a response. The network is optimised based on knowledge gained through the governing differential equation (DE) that describes the physics of the problem. Automatic differentiation [36] estimates the derivatives involved in the DE. Different deep neural network architecture has been proposed for PINN [37,38]. Wang et al. [39] investigated the limitation of the PINN training process via gradient descent and proposed an improved algorithm of gradient descent guided by a neural tangent kernel for resolving the issue. The gradient-enhanced PINNs are also used for structural dynamics [40]. If there exists model form error (i.e., the physics known is not exact), the final predicted results will be erroneous, as the modeling error is propagated to the PINN solution. There are several developments including the multi-fidelity framework [41,42] and other hybrid frameworks to eliminate model form errors [43]. However, these approaches need the generation of high-fidelity data from actual field measurements or laboratory experiments. Thus, a data-free approach is not possible when problems have model-form errors. A comprehensive review of the development of PINN in different fields can be found in Karniadakis et al. [44]. Applications of PINNs for structural response approximation can also be noted [45–48]. Physics-guided machine learning methods are developed for structural dynamics simulation [49] and for uncertainty quantification of nonlinear dynamical systems [50]. Various physics-informed machine learning approaches for reliability applications are reviewed by Xu et al. [51].

The PINN-based metamodeling approach for stochastic analysis was first proposed by Chakraborty [52]. The study suggested that random variables can be concatenated with spatiotemporal variables as inputs to the fully connected neural network. Latin hypercube sampling is employed to uniformly generate samples of random variables in the collocation points. However, the region near the failure plane is crucial for the accuracy of the reliability estimate [53]. Noting this, Zhang and Shafieezadeh [54] developed an adaptively trained PINN for reliability analysis (AT-PINN-RA) where the importance of random variables near the failure plane is gradually increased by an active learning approach. Besides simulation approaches, a FORM-based approach in combination with PINN (PINN-FORM) was recently developed by Meng et al. [55]. PINN-FORM does not require concatenating random variables with spatiotemporal variables but rather optimises values of random variables simultaneously with network parameters to obtain the MPP. Further to these studies, a generic PINN-based framework for the reliability assessment of multi-state systems [56], generative adversarial networks based PINN for system reliability [57], PINN for first-passage reliability estimation of structural dynamic systems [58] and reliability analysis of stochastic dynamical systems using PINN based probability density evolution method [59] can also be noted.

However, the existing studies on PINN for reliability analysis typically dealt with large failure probability (10^{-1}~10^{-3}) problems. In engineering risk assessment, rare events refer to occurrences of extreme system failures or accidents, which have a very low probability of occurrence but can lead to catastrophic consequences [60]. Examples include structural collapses of bridges, dams and buildings, aircraft accidents, and failure of facilities at nuclear power plants. Such engineering systems are typically designed to stringent reliability levels, making their failure exceptionally rare events [61]. In structural safety, it is critical to safeguard against failure resulting from extreme events due to uncertainties in external forces and structural factors [62]. Thus, the estimation of small failure probabilities is of paramount interest in structural reliability analysis [60]. However, estimating very low probabilities for such rare events through crude MCS requires an impractically large number of simulations and exorbitant computational costs. Conventional MCS methods are inadequate for efficiently modeling the failure in highly reliable systems [63]. There are a number of developments in metamodeling-based reliability analysis for estimating low failure probability [24,26,29,34,63–68]. However, no data-free or PINN-based approach to estimate low failure probability is available to the best of our knowledge. Therefore, this work caters to the timely demand for a data-free reliability analysis for low failure probability events.

The present study develops a computational framework to estimate small failure probabilities using a PINN-based metamodeling approach. The estimation of failure probabilities less than 10^{-5} is targeted in this study. In doing so, the importance sampling (IS) technique is integrated with PINN. It is to be noted that IS was previously utilized only for training PINN efficiently [69] but not for estimating low failure probability. In particular, the proposed approach consists of two stages. The first stage approximates the MPP using PINN-based metamodel and MCS samples. Whereas, the second stage obtains the failure probability based on the IS technique. The IS population is centred on the MPP approximated in the first stage. During the training of the PINN in the second stage, the samples from the IS population are selected batch-wise to ensure better accuracy at those samples as it directly affects the accuracy of failure probability. Thus, the present study proposed an effective sampling strategy for training of the physics-informed neural network to estimate low failure probabilities. This two-stage training strategy helps in getting accurate results with a limited number of iterations. The proposed two-stage physics-informed neural network approach is new and different from the existing physics-informed neural network approaches. Specifically, it is designed for estimating low failure probabilities. The effectiveness of the proposed two-stage PINN-based metamodeling approach is illustrated numerically with three structural reliability analysis problems.

2. Physics-informed neural network

PINN proposed by Raissi et al. [35] is an alternative numerical solver for different types of differential equations (DEs). The network architecture, training algorithm and advancement for reliability analysis are described briefly in the following under different sub-heads.

2.1. Network architecture

A fully connected neural network being the most common and simplest is used as the architecture of the PINN [54]. The network architecture can be expressed as follows,

$$\begin{aligned}
&\mathrm{O} = \psi_{L+1}(\mathbf{W}_{L+1}\mathbf{h}_L + \mathbf{b}_{L+1}) \\
&\mathbf{h}_L = \psi_L(\mathbf{W}_L\mathbf{h}_{L-1} + \mathbf{b}_L) \\
&\vdots \\
&\mathbf{h}_i = \psi_i(\mathbf{W}_i\mathbf{h}_{i-1} + \mathbf{b}_i) \\
&\vdots \\
&\mathbf{h}_1 = \psi_1(\mathbf{W}_1\mathbf{I} + \mathbf{b}_1)
\end{aligned} \tag{1}$$

where, $\mathbf{O}$, $\mathbf{I}$ and $\mathbf{h}_i$ are the output vector, input vector and output of hidden layers, respectively. There are L number of hidden layers. The output of (i-1)$^{\text{th}}$ layer is treated as input of ith layer, and the mapping is executed through a nonlinear activation function ψ_i, the weight matrix $\mathbf{W}_i$ and the bias vector $\mathbf{b}_i$. The input and output layers can be treated as 0^{th} and $(L+2)^{\text{th}}$ layers. For a compact representation, Eq. (1) is written as $\mathrm{O} = \mathrm{net}(\mathbf{I})$ where, net(•) represents a fully connected network. In the case of PINN, the input vector is composed of the spatial variables $\mathbf{x}$ and the temporal variable t. If there exists a governing DE $f(\mathbf{x}, t) = 0$ that has a solution $u(\mathbf{x}, t)$ then an approximation of the solution $\hat{u}(\mathbf{x}, t)$ is given by the output of PINN. Hence, a PINN model can be expressed as follows,

$$\hat{u}(\mathbf{x}, t) = \mathrm{net}(\mathbf{x}, t) \tag{2}$$

The activation functions are preselected for a PINN model and the values of $\mathbf{W}_i$ and $\mathbf{b}_i$ (also known as network parameters) are to be obtained through network training that is described in the next section.

2.2. Network training

Unlike training of a deep neural network, PINN for forward DE problems does not require any training data, i.e., data-free [54]. It requires the generation of collocation points where the violation of initial and boundary conditions and that of the DE are measured and minimized to obtain the network parameters. In doing so, the derivatives of $\hat{u}(\mathbf{x}, t)$ with respect to spatial and temporal variables are obtained by the automatic differentiation [36]. Using the value of these derivatives and $\hat{u}(\mathbf{x}, t)$, the deviation from the initial and boundary conditions and the error in the DE are calculated as follows,

$$\begin{aligned} L_{IC}(\mathbf{x}, t, u_{IC}) &= \hat{u}(\mathbf{x}, t)|_{IC} - u_{IC} \\ L_{BC}(\mathbf{x}, t, u_{BC}) &= \hat{u}(\mathbf{x}, t)|_{BC} - u_{BC} \\ L_{DE}(\mathbf{x}, t) &= f(\mathbf{x}, t) \end{aligned} \tag{3}$$

where, u_{IC} and u_{BC} are initial and boundary values of $u(\mathbf{x},t)$, respectively. The network parameters are learned by minimizing the mean squared error loss [35],

$$MSE = MSE_{IC} + MSE_{BC} + MSE_{DE} \tag{4}$$

where,

$$\begin{aligned} MSE_{IC} &= \frac{1}{N_{IC}} \sum_{i=1}^{N_{IC}} \left| L_{IC}\left(\mathbf{x}_{IC}^i, t_{IC}^i, u_{IC}^i\right)\right|^2 \\ MSE_{BC} &= \frac{1}{N_{BC}} \sum_{i=1}^{N_{BC}} \left| L_{BC}\left(\mathbf{x}_{BC}^i, t_{BC}^i, u_{BC}^i\right)\right|^2 \\ MSE_{DE} &= \frac{1}{N_{DE}} \sum_{i=1}^{N_{DE}} \left| L_{DE}\left(\mathbf{x}_{DE}^i, t_{DE}^i\right)\right|^2 \end{aligned} \tag{5}$$

In the above equation, $\{\mathbf{x}_{DE}^i, t_{DE}^i\}_{i=1}^{N_{DE}}$ denote the collocation points for $f(\mathbf{x}, t)$, $\{\mathbf{x}_{IC}^i, t_{IC}^i, u_{IC}^i\}_{i=1}^{N_{IC}}$ and $\{\mathbf{x}_{BC}^i, t_{BC}^i, u_{BC}^i\}_{i=1}^{N_{BC}}$ represent the initial and boundary training data on $u(\mathbf{x}, t)$, respectively.

2.3. PINN for reliability analysis

The use of PINN for reliability analysis is introduced by Chakraborty [52]. The limit state function (LSF) g of a structure can be expressed as,

$$g(\boldsymbol{\xi}) = u_c - u(\boldsymbol{\xi}) \tag{6}$$

where, $\boldsymbol{\xi}$ represents the random variables involved in the structure, and u_c is the allowable limit of the structural response u. The failure of the structure is represented by $g(\boldsymbol{\xi}) < 0$. The introduction of uncertainty in some structural parameters enables variation in the DE with these parameters, i.e., the DE becomes $f(\mathbf{x}, t, \boldsymbol{\xi}) = 0$. Subsequently, the objective of PINN has been changed to build a metamodel for u that not only depends on spatiotemporal variables $(\mathbf{x}, t)$ but also varies with random variables $\boldsymbol{\xi}$. Keeping this in mind, Chakraborty [52] proposed the concatenation of random variables $\boldsymbol{\xi}$ with spatiotemporal variables $(\mathbf{x}, t)$ as input variables to the PINN model, i.e.,

$$\hat{u}(\mathbf{x}, t, \boldsymbol{\xi}) = \mathrm{net}(\mathbf{x}, t, \boldsymbol{\xi}). \tag{7}$$

Following Eq. (7), the training points are modified as $\{\mathbf{x}_{DE}^i, t_{DE}^i, \boldsymbol{\xi}_{DE}^i\}_{i=1}^{N_{DE}}$, $\{\mathbf{x}_{IC}^i, t_{IC}^i, \boldsymbol{\xi}_{IC}^i, u_{IC}^i\}_{i=1}^{N_{IC}}$ and $\{\mathbf{x}_{BC}^i, t_{BC}^i, \boldsymbol{\xi}_{BC}^i, u_{BC}^i\}_{i=1}^{N_{BC}}$ for satisfying the DE, initial and boundary conditions, respectively. Accordingly, the errors described in Eq. (3) and the *MSE* loss described in Eqs. (4) and (5) are updated.

2.4. Elimination of loss terms for initial and boundary conditions

Further, the PINN model can be improved by incorporating the initial and boundary conditions into the input-output relation as follows [54],

$$\hat{u}(\mathbf{x}, t, \boldsymbol{\xi}) = u_{IC,BC} + B\mathrm{net}(\mathbf{x}, t, \boldsymbol{\xi}) \tag{8}$$

where, $u_{IC,BC}$ is a function that satisfies all the initial and boundary conditions, and the function $B = 0$ at points associated with these conditions. With the above modification, the scale difference arising from the different terms in the loss function, e.g., from the initial (L_{IC}) and boundary conditions (L_{BC}) are nullified. Eventually, the related loss terms MSE_{IC} and MSE_{BC} are no longer required and can be eliminated from the total loss *MSE* described in Eq. (4).

3. Proposed two-stage physics-informed neural network

The proposed PINN-based metamodeling approach for small failure probability problems is basically a two-stage training procedure of the network. The PINN model after the first stage of training approximates the most probable failure point (MPP), based on which an importance sampling (IS) population is built. The training in the second stage enhances the accuracy of the LSF at the samples of the IS population that are ultimately responsible for estimating the failure probability by the IS technique. Thus, the proposed approach is called the Physics-Informed Neural Network integrated with Importance Sampling (PINN-IS).

3.1. First stage

In the first stage, the entire input space is considered equally important for the accuracy of the PINN-based metamodel as the failure plane is not a known a priori. For this reason, n_{cp} uniform random samples are generated within the physical limits for each random variable. In the case of an unbounded random variable, uniform random samples are generated within five times the standard deviation σ from the mean μ [54]. For all spatial and temporal variables, n_{cp} uniform random samples are generated at each iteration within the range of their physical limits i.e., over the whole domain. Therefore, n_{cp} combinations of input variables are fed to the network at each iteration for calculating the DE loss. The network parameters are updated following the Adam optimization algorithm which is frequently used in different PINN applications. After 5000 iterations the lowest loss is recorded, and the iterations are stopped when the loss is less than the recorded loss. This new stopping criterion ensures a final network with parameters corresponding to the lowest loss in the entire training process.

The final network after the first-stage training is employed to approximate the LSF at N_{MCS} MCS samples. The failure point having the highest joint PDF can be treated as the MPP. Mathematically, the approximated MPP ($\boldsymbol{\mu}^{MPP}$) can be expressed as,

$$\boldsymbol{\mu}^{MPP} = \underset{\boldsymbol{\xi}^i}{arg\,max}\left\{ I\left[g\left(\boldsymbol{\xi}^i\right)\right] f_{\boldsymbol{\xi}}\left(\boldsymbol{\xi}^i\right)\right\} \tag{9}$$

where, $\boldsymbol{\xi}^i$ represents the ith sample with a joint PDF $f_{\boldsymbol{\xi}}(\boldsymbol{\xi}^i)$. The indicator function, $I[g(\boldsymbol{\xi})]$ is equal to 1 for $g(\boldsymbol{\xi}) < 0$ and 0, otherwise. The approximated MPP (say, $\boldsymbol{\mu}^{MPP}$) is used as the centre of the quasi-optimal density function for an IS population. If there is no failure point found from N_{MCS} MCS samples, then the MCS sample with the lowest magnitude of LSF will be considered as the centre. N_{IS} importance samples are generated from a multi-normal distribution with MPP as the mean vector and original standard deviation as the standard deviation for each random variable [70,71]. Then the joint PDF for the importance sampling density function, f_{IS} at any point $\boldsymbol{\xi}$ is obtained as,

$$f_{IS}(\boldsymbol{\xi}) = \prod_{k=1}^{n} \phi\left(\frac{\xi_k - \mu_k^{MPP}}{\sigma_k}\right) \tag{10}$$

where, n is the dimension of $\boldsymbol{\xi}$ and σ_k represents the original standard deviation of ξ_k. If any random variable follows a truncated distribution, then the corresponding normal distribution is also truncated by its original truncation limits. It can be noted that the first stage involves searching for a suitable centre for a quasi-optimal IS population, not an accurate MPP. Subsequently, the IS technique will estimate failure probability and therefore the accuracy of MPP estimation does not affect the accuracy of the failure estimate in a single-MPP problem [66]. However, the proposed method is not suitable for a multi-MPP problem. In detail, only one MPP with the highest joint probability density will be selected in case of multi-MPP problems. Subsequently, only one IS population around this MPP will be generated. Therefore, the contributions from the failure region far from the selected MPP will be neglected. In addition, it is also difficult to obtain a convergent MPP from the MCS sampling pool for the high-dimensional problem. Thus, the proposed approach is not suitable for multi-MPP or high-dimensional problems.

3.2. Second stage

The training in the second stage primarily aims to improve the accuracy of the prediction at N_{IS} importance samples. For this, the DE loss in these samples is minimized. However, the calculation of DE loss at N_{IS} importance samples for each iteration increases the computation cost significantly. The computation can be accelerated if DE loss is calculated for a smaller number of samples. To do this, N_{IS} importance samples are split into 100 batches of n_{100} points (i.e., $n_{100} = N_{\mathrm{IS}}/100$). At each iteration, one batch consisting of n_{100} samples is selected for random variables and n_{100} uniform random samples are generated for each spatiotemporal variable. Then, samples of random variables and spatiotemporal variables are concatenated to calculate the DE loss. Based on the calculated DE loss, the network parameters are updated at each iteration following the Adam optimizer. After 5000 iterations, the same stopping criterion as introduced in the first stage is applied. The final PINN after the second-stage training is employed to approximate the LSF at N_{IS} importance samples. The failure probability is estimated based on the IS technique as [72],

$$P_f = \frac{1}{N_{IS}} \sum_{i=1}^{N_{IS}} I\left[g\left(\boldsymbol{\xi}^i\right)\right] \frac{f_{\xi}\left(\boldsymbol{\xi}^i\right)}{f_{IS}\left(\boldsymbol{\xi}^i\right)} \tag{11}$$

where, f_ξ and f_{IS} are the joint PDFs for the actual input space and the generated IS population, respectively. The size of the IS sampling pool should be such that the coefficient of variation (COV) of the estimated failure probability is below an acceptable value. The acceptable COV for the estimated failure probability is chosen as 0.1 in the present study.

3.3. Outline of PINN-IS

It can be noted that the fully connected neural network structure is adopted for the present study, the same as that used by Chakraborty [52] and AT-PINN-RA [54]. Like Chakraborty [52], no adaptive sampling approach is adopted in the first stage of the algorithm. However, new training points are generated at each iteration instead of generating a large set of collocation points and calling them by mini-batches. Unlike AT-PINN-RA [54], the first stage treated the whole input space as equally important to find an approximate MPP. The accuracy of the PINN model at the first stage is not important near the failure plane as it is not employed for reliability estimation by any simulation technique. Therefore, adaptive sampling is not necessary at this stage rather the MPP is to be approximated appropriately. Unlike PINN-FORM [55], the approximated MPP is not utilized to obtain the reliability index or an equivalent failure probability but is used as the centre for generating a quasi-optimal IS density function. Finally, the failure probability is estimated by the IS technique using the LSF prediction of the PINN model obtained after the training in the second stage. Therefore, training points are selected batch-wise from the IS population at each iteration in the second stage to improve the accuracy of the prediction at those points. Hence, the proposed approach is significantly different from the existing PINN approaches for reliability analysis. The step-by-step procedure is outlined in Algorithm 1.

Algorithm 1. Step-by-step procedure for implementing the proposed two-stage PINN framework to determine low failure probability events

1) Initialize the PINN model parameters $\mathbf{W}_i$ and $\mathbf{b}_i$.
2) Generate n_{cp} uniform random samples of both the spatiotemporal and random variables in the range of their physical limits or $[\mu - 5\sigma, \mu + 5\sigma]$.
3) Scale variables between −1.0 and 1.0. Concatenate all the variables as $\{\mathbf{x}_{DE}^i, t_{DE}^i, \boldsymbol{\xi}_{DE}^i\}_{i=1}^{n_{cp}}$ and feed the network.
4) Calculate the DE loss at $\{\mathrm{x}_{\mathrm{DE}}^i, \mathrm{t}_{\mathrm{DE}}^i, \xi_{\mathrm{DE}}^i\}_{i=1}^{\mathrm{n_{cp}}}$ and obtain the total loss MSE described in Eq. (4). Following sec. 2.4 and Eq. (8), update input-output relation to automatically satisfy initial and/or boundary conditions, as a consequence, $MSE_{IC} = MSE_{BC} = 0$ and $MSE = MSE_{DE}$.
5) Update $\mathbf{W}_i$ and $\mathbf{b}_i$ by Adam optimization algorithm. Go to 2) if iteration <5000.
6) Record the lowest MSE among all previous iterations as MSE_{stage1}^{lowest} if iteration = 5000.
7) if iteration >5000 and $MSE > MSE_{stage1}^{lowest}$, Go to 2), otherwise, end of training.

Obtain the first-stage PINN model.

8) Generate N_{MCS} MCS samples according to the PDF of random variables.
9) Employ the first-stage PINN model to find the approximated MPP $\boldsymbol{\mu}^{MPP}$ as described in Eq. (9).
10) Generate N_{IS} importance samples by a multi-normal distribution centred at $\boldsymbol{\mu}^{MPP}$ as defined in Eq. (10).
11) Split N_{IS} importance samples into 100 batches of n_{100} points.
12) Initialize the second-stage PINN model parameters $\mathbf{W}_i$ and $\mathbf{b}_i$.
13) Select one batch of n_{100} importance samples for random variables and generate n_{100} uniform random samples for each spatiotemporal variable.
14) Scale variables between −1.0 and 1.0. Concatenate samples of all variables and feed the second-stage PINN.
15) Calculate MSE.
16) Update $\mathbf{W}_i$ and $\mathbf{b}_i$ by Adam optimization algorithm. Go to 13) if iteration <5000.
17) Record the lowest MSE among all previous iterations of the second stage iterations as MSE_{stage2}^{lowest}, if iteration = 5000.
18) if iteration >5000 and $MSE > MSE_{stage2}^{lowest}$, Go to 13), otherwise, end of training.

Obtain the second-stage PINN model.

19) Employ the second-stage PINN model to approximate the LSF at $\mathrm{N_{IS}}$ importance samples.
20) Estimate P_f based on the IS technique as formulated in Eq. (11).

4. Numerical study

The proposed two-stage PINN-based metamodeling approach for reliability analysis involving small failure probability is illustrated by considering three structural analysis examples. The first example considers a straight bar subjected to an axial load. The deflection of a cantilever beam under a uniform distributed load is studied in the second example. The last example is the deflection of a thin square plate under a non-uniform loading. The resulting unique DEs in these three examples are solved by the proposed two-stage PINN approach. Both ordinary and partial DEs are considered in these example problems. The PINN consists of five fully connected hidden layers with each layer having 50 neurons and the sigmoid activation function is employed. However, it is well known that the sigmoid activation saturates at the two ends and gives rise to the vanishing gradient problem. The highest gradient of the sigmoid activation is observed at zero and then gradually decreases in both directions. The input of the activation function should be closer to zero to get a higher gradient value. Following this, the proposed algorithm scales the input variables between −1.0 and 1.0 to ensure a significant gradient value. Adam algorithm with a learning rate of 0.001 is employed to optimize the network parameters of the PINN.

The values of n_{cp}, N_{MCS} and N_{IS} are taken as 500, one million and 50,000, respectively. The results are also obtained by the MCS technique followed by an IS technique using the analytical solutions to validate the accuracy of the proposed approach.

4.1. A straight bar subjected to an axial load

A straight bar shown in Fig. 1 is taken as the first example. The left end of the bar is fixed, and an axial force F acts on the right end. The cross-sectional area A, the Young's modulus E and F follow triangular probability distributions. Table 1 shows the distribution parameters of F, A and E. The following differentiation equation describes the problem,

$$\frac{du}{dx} - \frac{F}{AE} = 0 \tag{12}$$

where, u is the displacement of the bar at a distance x from the fixed end. The initial condition of the problem is stated as follows,

$$u = 0 \text{ at } x = 0 \tag{13}$$

The LSF is defined as follows,

$$g = u_{\max} - (u)_{x=5} \tag{14}$$

where, $u_{\max}$ is the maximum allowable displacement of the bar.

In this problem, there are four input variables (one spatial variable x, and three random variables F, A and E) and one output variable for approximating the displacement u. The network can be expressed as,

$$\hat{u} = \mathrm{net}(x, F, A, E) \tag{15}$$

To automatically satisfy the initial condition, the above relation can be modified as follows,

$$\hat{u} = x\mathrm{net}(x, F, A, E) \tag{16}$$

Therefore, only the loss term related to DE is to be minimized. In the proposed PINN-IS approach, 500 collocation points are generated for the spatial variable x between 0.0 and 5.0 at each iteration. For three random variables, 500 samples are generated within their distribution truncation limits. Following the algorithm described in section 3, a PINN model is finalized in the first stage of the algorithm. Based on the PINN model, u at $x = 5$ m is approximated in one million MCS points to get the MPP. Then, 50,000 importance samples are generated for three random variables and divided into 100 batches each containing 500 samples. In the second stage of the algorithm, samples of one batch are concatenated with 500 uniform random samples of x at each iteration to train the PINN. Once, the PINN model is converged, u at $x = 5$ m is obtained for 50,000 importance samples and P_f is calculated based on Eq. (11). Results obtained by the proposed PINN-IS approach are labelled as 'Two-stage PINN-IS'. Using the analytical solution, the value of u at $x = 5$ m is obtained for one million MCS samples to get an approximate MPP. Based on the MPP, 50,000 importance samples are generated to calculate P_f using Eq. (11). This reliability estimation approach is denoted by the 'MCS + IS' and its results are considered as the benchmark. The proposed algorithm and 'MCS + IS' are identical in selecting simulation samples (for MCS and IS techniques) and reliability estimation methods. In particular, both methods first select an approximate MPP from an

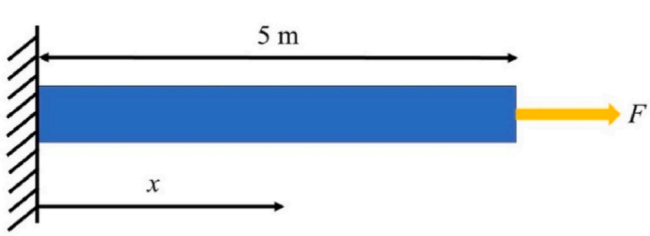

Fig. 1. A straight bar subjected to an axial load.

Table 1
The triangular distribution parameters of random variables of the straight bar.

Random Variable	Mean	SD	Lower bound	Upper bound
F	10.0×10^3 N	1.0×10^3 N	7.550×10^3 N	12.449×10^3 N
A	0.0001 m^2	0.00001 m^2	0.755×10^{-4} m^2	1.245×10^{-4} m^2
E	2.06×10^{11} N/m^2	0.15×10^{11} N/m^2	1.693×10^{11} N/m^2	2.427×10^{11} N/m^2

MCS pool for the subsequent IS technique. The only difference is that 'MCS + IS' uses the actual LSF and the proposed approach employs an approximate LSF. For this reason, the 'MCS + IS' has been used for benchmarking results and not as a competitive method. As the existing literature for reliability analysis using the PINN model uses single-stage training and is not suitable for small failure probability problems, the PINN model converged after the first stage of the proposed approach is also employed to estimate the failure probability based on the IS technique and this approach is labelled as 'Single-stage PINN-IS'. However, numerous metamodel-based algorithms are available to solve the problem with a small failure probability. These methods are data-driven, which means they require to be trained with input-output data and hence, involve actual function evaluations. Active learning-based adaptive Kriging combined with IS or AK-IS [66] being a well-noted approach among them is also considered for comparison. The conventional IS technique where MPP is obtained by FORM is also employed to estimate failure probability. To study the performances of the FORM, conventional IS, AK-IS, 'MCS + IS', 'Single-stage PINN-IS' and 'Two-stage PINN-IS' approaches in different failure probability ranges, the value of u_{max} in the LSF is varied. IS, AK-IS, 'MCS + IS', 'Single-stage PINN-IS' and 'Two-stage PINN-IS' approaches are repeated 10 times to study the variations in the results due to the use of pseudo-random numbers for the generation of random samples. For a meaningful comparison, the MCS populations used by 'MCS + IS', 'Single-stage PINN-IS' and 'Two-stage PINN-IS' approaches are identical in each case of repetition. The different statistics of 10 repetition results of IS, AK-IS, 'MCS + IS', 'Single-stage PINN-IS' and 'Two-stage PINN-IS' approaches are depicted by boxplots in Fig. 2(a) and (b) and (c) for $u_{max} = 4.4 \times 10^{-3}$ m, 4.5×10^{-3} m and 4.6×10^{-3} m, respectively. The variations of IS, AK-IS, 'MCS + IS' and 'Two-stage PINN-IS' approaches are comparable or similar. Larger variations of 'Single-stage PINN-IS' results are observed than the other approaches. Table 2 shows the result of FORM, the average P_f values estimated by the IS, AK-IS, 'MCS + IS', 'Single-stage PINN-IS' and 'Two-stage PINN-IS' approaches for different values of u_{max} and their corresponding number of actual function evaluations required. Results of IS, AK-IS, 'MCS + IS' and 'Two-stage PINN-IS' approaches are very close to each other, but 'Two-stage PINN-IS' requires no actual function evaluation. The absolute percentage errors of 'Single-stage PINN-IS' and 'Two-stage PINN-IS' approaches with respect to 'MCS + IS' are also reported in the table. The average result of 10 'MCS + IS' repetitions is considered as the reference to calculate the absolute percentage errors of the average results of the other two approaches. In the case of 'Single-stage PINN-IS', high errors are observed for estimating lower P_f values than 10^{-5}. On the other hand, the 'Two-stage PINN-IS' approach produces very accurate results (errors are in the range of 0.32%–5.67%) for all three ranges of P_f values. This observation indicates the efficiency of the proposed two-stage PINN model for estimating small failure probabilities. This example problem with a different parameter setting was previously studied by Meng et al. [55]. Their PINN-FORM approach took 0.5 million iterations to estimate a large failure probability value. Whereas the proposed PINN-IS approach produces accurate results using about 10,000 iterations for a much smaller (10^{-5} to 10^{-7}) failure probability.

The problem statement is modified to study the performance of the

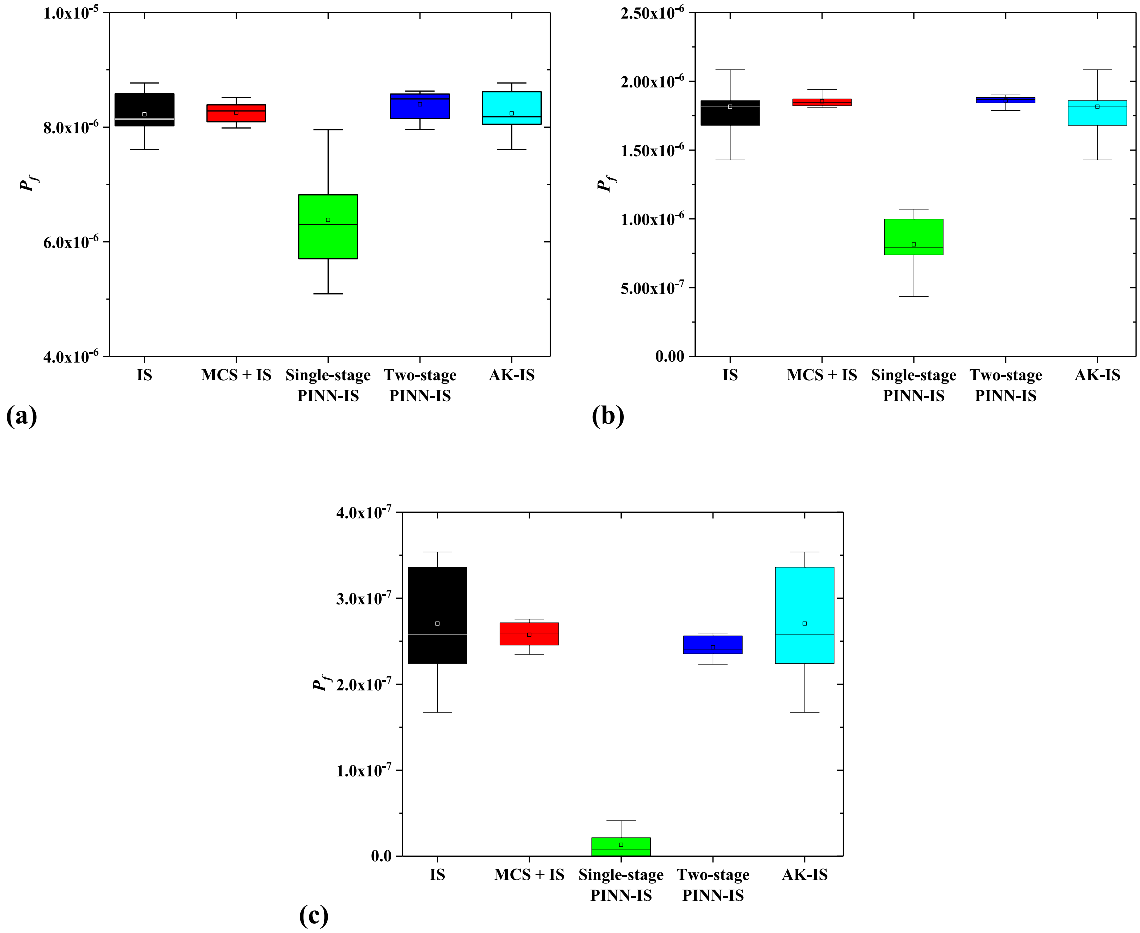

Fig. 2. Summary of statistical observation on results obtained from repetitions of different reliability analysis approaches for (a) $u_{max} = 4.4 \times 10^{-3}$ m, (b) $u_{max} = 4.5 \times 10^{-3}$ m and (c) $u_{max} = 4.6 \times 10^{-3}$ m.

Table 2
Results of reliability analysis for the straight bar.

Reliability approach	P_f [no. of function evaluations] and (absolute error in %)		
	$u_{max} = 4.4 \times 10^{-3}$ m	$u_{max} = 4.5 \times 10^{-3}$ m	$u_{max} = 4.6 \times 10^{-3}$ m
FORM	3.594×10^{-4} [37]	3.057×10^{-4} [37]	2.272×10^{-4} [37]
IS	8.224×10^{-6} [37 + 50,000]	1.816×10^{-6} [37 + 50,000]	2.705×10^{-7} [37 + 50,000]
AK-IS	8.240×10^{-6} [37 + 0]	1.816×10^{-6} [37 + 0]	2.705×10^{-7} [37 + 0]
MCS + IS	8.253×10^{-6} [10^6 + 50,000]	1.854×10^{-6} [10^6 + 50,000]	2.575×10^{-7} [10^6 + 50,000]
Single-stage PINN-IS	6.383×10^{-7} [nil] (92.27%)	8.141×10^{-7} [nil] (56.01%)	1.328×10^{-8} [nil] (94.84%)
Two-stage PINN-IS	8.397×10^{-6} [nil] (1.74%)	1.860×10^{-6} [nil] (0.32%)	2.429×10^{-7} [nil] (5.67%)

proposed approach for high-dimensional problems. In doing so, the E is assumed to be a function of N independent random variables. If λ_i represents the ith independent random variable, then E is expressed as,

$$E = E_1 + \frac{E_2}{7}\sqrt{\frac{21}{N}}\sum_{i=1}^{N}\lambda_i \tag{17}$$

where, $E_1 = 2.07 \times 10^{11}$ N/m^2 and $E_2 = 2.0 \times 10^{10}$ N/m^2. Each of λ_i follows a triangular probability distribution with zero mean and is bounded between -1.0 and 1.0. The values of F, A and u_{max} are taken as 10×10^3 N, 0.0001 m^2 and 2.72×10^{-3} mm, respectively for reliability analysis. After the modification, the problem has N+1 variables (1 spatial and N random variables). Two different values of N (i.e., 12 and 21) are considered to illustrate how the dimensionality affects the performance. The reliability results are obtained by IS, AK-IS, 'MCS + IS' and the proposed methods, which have ten repetitions, like the previous case. The average values of the failure estimates and the total number of function evaluations required by ten repetitions are reported in Table 3. Results of IS, AK-IS, 'MCS + IS' and 'Two-stage PINN-IS' approaches are very close to each other for the 12-dimensional case. A higher difference in average reliability results by these approaches is observed for the 21-dimension case compared to the 12-dimension case. The result produced by the proposed 'Two-stage PINN-IS' lies between IS and 'MCS + IS' results, whereas AK-IS overestimates the failure probability for the 21-dimension case. Poor performance of 'Single-stage PINN-IS' is

Table 3
Results of reliability analysis for the high-dimension cases of the straight bar.

Reliability approach	P_f [no. of function evaluations] and (absolute error in %)	
	$N = 12$	$N = 21$
FORM	2.272×10^{-5} [40]	2.547×10^{-5} [67]
IS	3.320×10^{-6} [40 + 50,000]	4.795×10^{-6} [67 + 50,000]
AK-IS	3.374×10^{-6} [40 + 0.1[a]]	5.397×10^{-6} [67 + 2.8[a]]
MCS + IS	3.332×10^{-6} [10^6 + 50,000]	4.372×10^{-6} [10^6 + 50,000]
Single-stage PINN-IS	7.201×10^{-9} [nil] (99.78%)	2.803×10^{-7} [nil] (93.59%)
Two-stage PINN-IS	3.360×10^{-6} [nil] (0.84%)	4.509×10^{-6} [nil] (3.13%)

[a] The average value of ten repetitions is shown up to the first decimal place.

observed in both cases. The summary of statistical observation on results obtained from repetitions of different reliability analysis approaches for the high-dimension case of the straight bar is shown in Fig. 3. Variation in the proposed 'Two-stage PINN-IS' results increases with dimensionality. One possible reason for this variation is the process of MPP evaluation. The IS pool for the proposed 'Two-stage PINN-IS' is based on the MPP obtained by the 'Single-stage PINN-IS' which is largely affected by the performance of 'Single-stage PINN-IS'. Moreover, it is also difficult to obtain a convergent MPP from the MCS pool for high-dimensional problems. On the other hand, AK-IS results are based on a fixed MPP obtained by FORM. For this, AK-IS results have lesser variation compared to the proposed 'Two-stage PINN-IS' results. Hence, further improvement of the proposed algorithm for higher dimension problems should be explored to reduce the variation in results. This aspect is considered as a future scope of study.

4.2. A cantilever beam under a uniform distributed load

The second example is a cantilever beam (shown in Fig. 4) with a uniformly distributed load w over it. The length of the beam l is taken as 2 m. The Young's modulus E, the moment of inertia I and w follow truncated normal random distributions. The distribution parameters of w, E and I are shown in Table 4. The following DE governs the deflection of the cantilever beam due to a uniform loading,

$$EI\frac{d^2u}{dx^2}-\frac{w(l-x)^2}{2}=0 \tag{18}$$

where, u is the deflection of the beam at distance x from the fixed end. The initial conditions are zero slope and no deflection at the fixed end,

$$\frac{du}{dx}=0 \text{ and } u=0 \text{ at } x=0 \tag{19}$$

The LSF is defined as follows,

$$g=u_{\max}-(u)_{x=l} \tag{20}$$

where, $u_{\max}$ is the maximum allowable deflection at the free end of the beam (i.e., $x = 2$ m).

Like the previous example, there are four input variables (one spatial variable x, and three random variables w, E and I) and one output variable for approximating the beam deflection u, i.e.,

$$\hat{u}=\mathrm{net}(x,w,E,I) \tag{21}$$

This input-output relation is modified to automatically satisfy the initial conditions stated in Eq. (19) as follows,

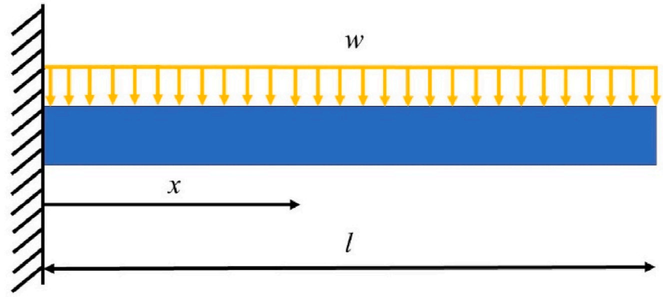

Fig. 4. A cantilever beam under a uniform distributed load.

Table 4
The distribution parameters of truncated normal random variables of the cantilever beam.

Random Variable	Mean	SD	Lower bound	Upper bound
w	2×10^3 N/m	0.2×10^3 N/m	1.4×10^3 N/m	2.6×10^3 N/m
I	1.0×10^{-5} m^4	0.1×10^{-5} m^4	0.7×10^{-5} m^4	1.3×10^{-5} m^4
E	2.0×10^{11} N/m^2	0.15×10^{11} N/m^2	1.55×10^{11} N/m^2	2.45×10^{11} N/m^2

$$\hat{u}=x^2\mathrm{net}(x,w,I,E) \tag{22}$$

The 'MCS + IS', 'Single-stage PINN-IS' and 'Two-stage PINN-IS' approaches are employed to estimate the P_f for three different values of u_{max} in the LSF. Statistics of ten repetition results by IS, AK-IS, 'MCS + IS', 'Single-stage PINN-IS' and 'Two-stage PINN-IS' approaches are depicted in Fig. 5(a) and (b) and (c) by boxplots for $u_{max} = 3.9 \times 10^{-3}$ m, 4.0×10^{-3} m and 4.2×10^{-3} m, respectively. The ranges of IS, AK-IS, 'MCS + IS' and 'Two-stage PINN-IS' are observed to be close to each other while that of 'Single-stage PINN-IS' are away from the other approaches. The result of FORM and the average results of ten repetitions with their required number of actual function evaluations of the IS, AK-IS, 'MCS + IS', 'Single-stage PINN-IS' and 'Two-stage PINN-IS' approaches are reported in Table 5. Without any actual function evaluation, the 'Two-stage PINN-IS' approach produces very similar results as IS, AK-IS and 'MCS + IS'. The absolute percentage errors of the 'Single-stage PINN-IS' and 'Two-stage PINN-IS' approaches are compared in the table. In the case of 'Two-stage PINN-IS', about 3%–5% errors are observed for estimating failure probability in the range of 10^{-5} to 10^{-6}.

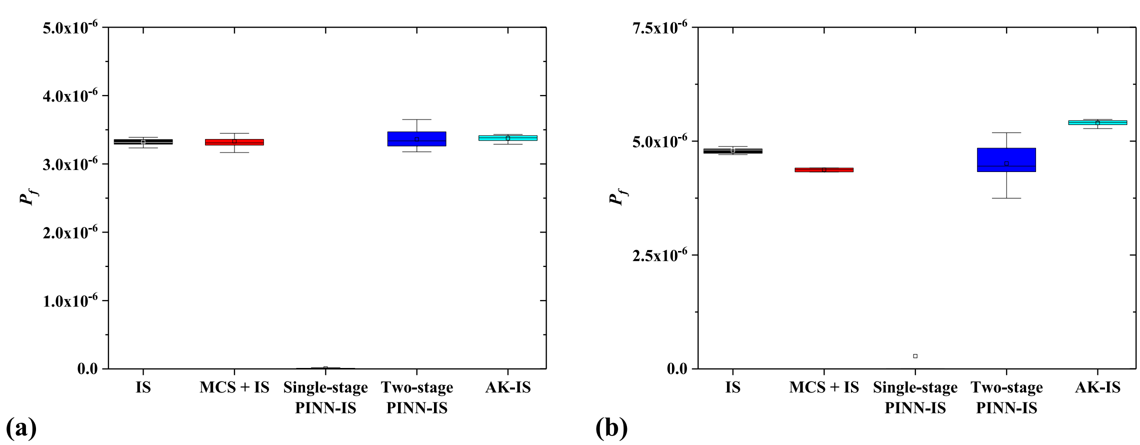

Fig. 3. Summary of statistical observation on results obtained from repetitions of different reliability analysis approaches for the high-dimension case of the straight bar.

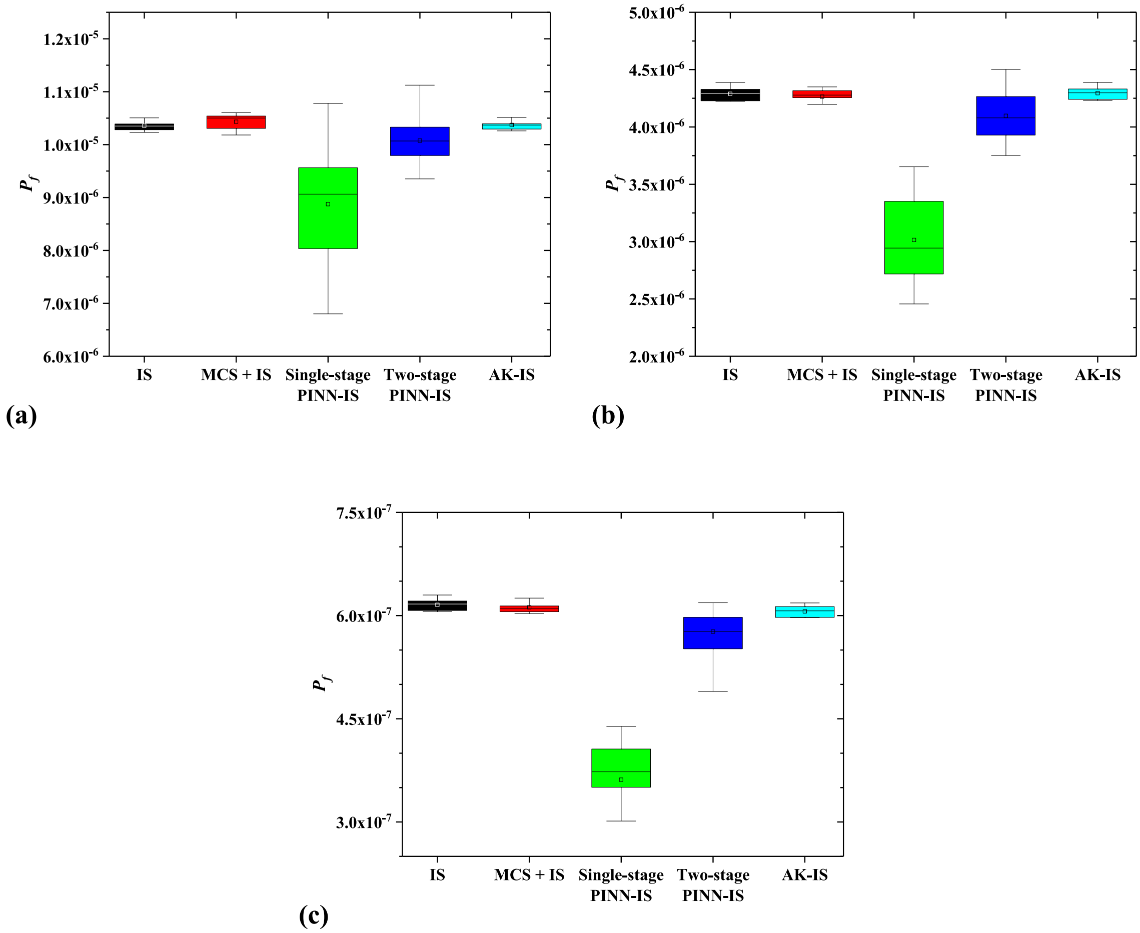

Fig. 5. Summary of statistical observation on results obtained from repetitions of different reliability analysis approaches for (a) $u_{max} = 3.9 \times 10^{-3}$ m, (b) $u_{max} = 4.0 \times 10^{-3}$ m and (c) $u_{max} = 4.2 \times 10^{-3}$ m.

Table 5
Results of reliability analysis for the cantilever beam.

Reliability approach	P_f, [no. of function evaluations] and (absolute error in %)		
	$u_{max} = 3.9 \times 10^{-3}$ m	$u_{max} = 4.0 \times 10^{-3}$ m	$u_{max} = 4.2 \times 10^{-3}$ m
FORM	2.402×10^{-5} [29]	1.644×10^{-5} [37]	5.180×10^{-15} [37]
IS	1.036×10^{-5} [29 + 50,000]	4.289×10^{-6} [37 + 50,000]	6.156×10^{-7} [37 + 50,000]
AK-IS	1.037×10^{-5} [29 + 0]	4.295×10^{-6} [37 + 0]	6.061×10^{-7} [37 + 0]
MCS + IS	1.043×10^{-5} [10^6 + 50,000]	4.264×10^{-6} [10^6 + 50,000]	6.120×10^{-7} [10^6 + 50,000]
Single-stage PINN-IS	8.875×10^{-6} [nil] (14.93%)	3.015×10^{-6} [nil] (29.31%)	3.615×10^{-7} [nil] (40.93%)
Two-stage PINN-IS	1.007×10^{-5} [nil] (3.42%)	4.097×10^{-6} [nil] (3.94%)	5.767×10^{-7} [nil] (5.76%)

However, the errors of results by ‘Single-stage PINN-IS’ are significantly high and rapidly increase for lower failure probabilities.

4.3. A thin square plate with a non-uniform loading

A thin square plate shown in Fig. 6 is considered as the final example. The four sides of the plate are simply supported. The thickness of the plate (t) is 0.05 m, and the length of each side is π m. A spatially varying non-uniform load $q_0 \sin x \sin y$ is applied over the plate. The governing partial DEs of the plate are stated as follows,

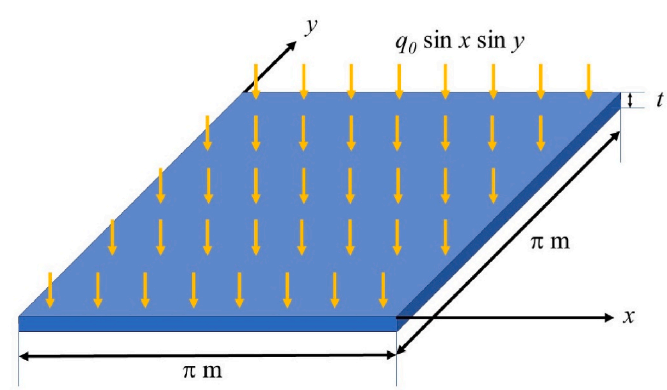

Fig. 6. A thin square plate with a non-uniform loading.

$$\frac{\partial^4 u}{\partial x^4} + \frac{\partial^4 u}{\partial x^2 \partial y^2} + \frac{\partial^4 u}{\partial y^4} - \frac{q_0 \sin x \sin y}{D} = 0 \tag{23}$$

where D is the bending stiffness of the plate and is defined as follows:

$$D = \frac{Et^3}{12(1-\nu^2)} \tag{24}$$

Here, t is the thickness of the plate, E and ν are the Young’s modulus and the Poisson ratio of the plate material, respectively. In this example, $t = 0.05$ m is taken, and q_0, E and ν are considered as random variables following truncated normal distributions. The distribution parameters are shown in Table 6. The boundary conditions of the plate are described as follows,

$$u = 0 \text{ and } \frac{\partial^2 u}{\partial x^2} = 0 \text{ at } x = 0, \pi$$
$$u = 0 \text{ and } \frac{\partial^2 u}{\partial y^2} = 0 \text{ at } y = 0, \pi \tag{25}$$

The LSF for the plate deflection is defined as follows,

$$g = u_{\max} - (u)_{x=\pi/2, y=\pi/2} \tag{26}$$

where, $u_{\max}$ is the maximum allowable deflection at the mid-point of the plate, i.e., at $x = \pi/2$ m and $y = \pi/2$ m.

In this problem, there are five input variables (two spatial variables x and y, and three random variables q_0, E and ν) and one output variable for approximating the displacement u. The network can be expressed as,

$$\hat{u} = \text{net}(x, y, q_0, E, \nu) \tag{27}$$

To automatically satisfy the conditions described in Eq. (25), the input-output relation can be modified as follows,

$$\hat{u} = \sin x \sin y \text{net}(x, y, q_0, E, \nu) \tag{28}$$

The performances of the 'MCS + IS', 'Single-stage PINN-IS' and 'Two-stage PINN-IS' are studied for three different values of u_{max} that yield different ranges of P_f values. For each case, ten repetitions are performed. Different statistics of ten repetitions by IS, AK-IS, 'MCS + IS', 'Single-stage PINN-IS' and 'Two-stage PINN-IS' approaches are summarised by boxplots in Fig. 7(a) and (b) and (c) for $u_{max} = 0.2$ m, 0.21 m and $u_{max} = 0.22$ m, respectively. Wide variations of results by 'Single-stage PINN-IS' are observed while that of IS, AK-IS, 'MCS + IS' and 'Two-stage PINN-IS' approaches are comparable. The result of FORM and the average results of IS, AK-IS, 'MCS + IS', 'Single-stage PINN-IS' and 'Two-stage PINN-IS' approaches are shown in Table 7. The average results of IS, AK-IS, 'MCS + IS' and 'Two-stage PINN-IS' approaches are very close to each other. However, IS, AK-IS and 'MCS + IS' approaches require a large number of actual function evaluations. The absolute percentage errors of 'Single-stage PINN-IS' and 'Two-stage PINN-IS' approaches are also reported in the table. In the case of 'Single-stage PINN-IS', the error increases from 4% to 40% for reducing the order of failure probability from 10^{-5} to 10^{-6}. Whereas, the errors in the case of 'Two-stage PINN-IS' increase from 1% to 2% only for the same decrement of the P_f value which demonstrates its efficacy for estimating low failure probability. Like the first example, the present example with a different parameter setting was previously also studied by Meng et al. [55] where 0.2 million iterations are required by their (PINN-FORM) approach to estimate a large failure probability value. However, our proposed approach can effectively estimate a low failure probability ($<10^{-6}$) using only about 10,000 iterations.

5. Conclusions

In the present study, a two-stage physics-informed neural network (PINN) based metamodeling approach is developed to accurately estimate rare events with low failure probability. The first stage of the proposed approach is involved in training a PINN model appropriately to obtain an approximate most probable failure point (MPP) from a Monte Carlo simulation (MCS) population, and the second stage is responsible for the efficient training of another PINN model to approximate the limit state function (LSF) at samples of IS population centred on the approximated MPP. Finally, the failure probability is estimated by the IS technique. To compare the accuracy, the MPP from an MCS population and subsequently the failure probability based on the IS technique are also obtained by utilizing the actual LSF based on the analytical solution. The results from this approach are considered as the benchmark.

To the best of our knowledge, there is no existing PINN approach for small failure problems. Therefore, the PINN model obtained in the first stage is also employed to estimate failure probability by the IS technique and results (labelled by Single-stage PINN-IS) are compared with the proposed Two-stage PINN-IS approach. Three structural reliability analysis problems involving small failures are investigated numerically. All the problems are studied for a wide range of failure probabilities to test the robustness of the approaches. The results of single-stage PINN-IS produce large errors in small failure probabilities whereas the results of the proposed two-stage PINN-IS are close to that of the benchmark. This clearly indicates that the model training in the second stage is particularly effective for estimating small probabilities. The key advantages of the proposed PINN-IS metamodeling approach include the following,

- Ability to perform reliability analysis without a single evaluation of the actual LSF i.e., data-free.
- Capability of estimating failure probabilities less than 10^{-5} with a satisfactory level of accuracy.
- Competency to train the PINN models with only about 10,000 iterations.
- Provision to deal with any probability distribution of random variables.
- Flexibility of incorporating any advancement of the IS technique and use of improved network architecture (e.g., convolutional neural networks and recurrent neural networks)

The proposed approach opens up a new paradigm of data-free reliability analysis of structural systems having low failure probability and demonstrates the efficacy of PINN-integrated IS. As the proposed algorithm is generic in nature, the application is not only limited to structures but can also be extended to solve low failure probability problems involving complex physics such as crack propagation, fluid mechanics, molecular dynamics etc. In the present study, three basic structural elements (bar, beam and plate) are investigated considering uncorrelated random variables. PINN-based reliability analysis for correlated random variables will be considered in future studies for solving more realistic engineering problems. Further, there is scope for enhancement of the proposed algorithm for higher dimension problems and problems with multiple MPPs. Future work can be extended to complex structures and time-dependent reliability analysis by employing advanced neural architectures, such as convolutional neural networks and recurrent neural networks.

Table 6
The distribution parameters of the truncated normal random variables of the thin square plate.

Random Variable	Mean	SD	Lower bound	Upper bound
q_0	0.5×10^6 N/m^2	0.2×10^6 N/m^2	0.0 N/m^2	1.0×10^6 N/m^2
E	2.0×10^{11} N/m^2	0.2×10^{11} N/m^2	1.4×10^{11} N/m^2	2.6×10^{11} N/m^2
ν	0.3	0.1	0.0	0.6

CRediT authorship contribution statement

Atin Roy: Writing – original draft, Visualization, Validation, Software, Methodology, Formal analysis, Data curation, Conceptualization. **Tanmoy Chatterjee:** Writing – review & editing, Supervision, Conceptualization. **Sondipon Adhikari:** Writing – review & editing, Supervision, Resources.

Declaration of competing interest

The authors declare that they have no known competing financial

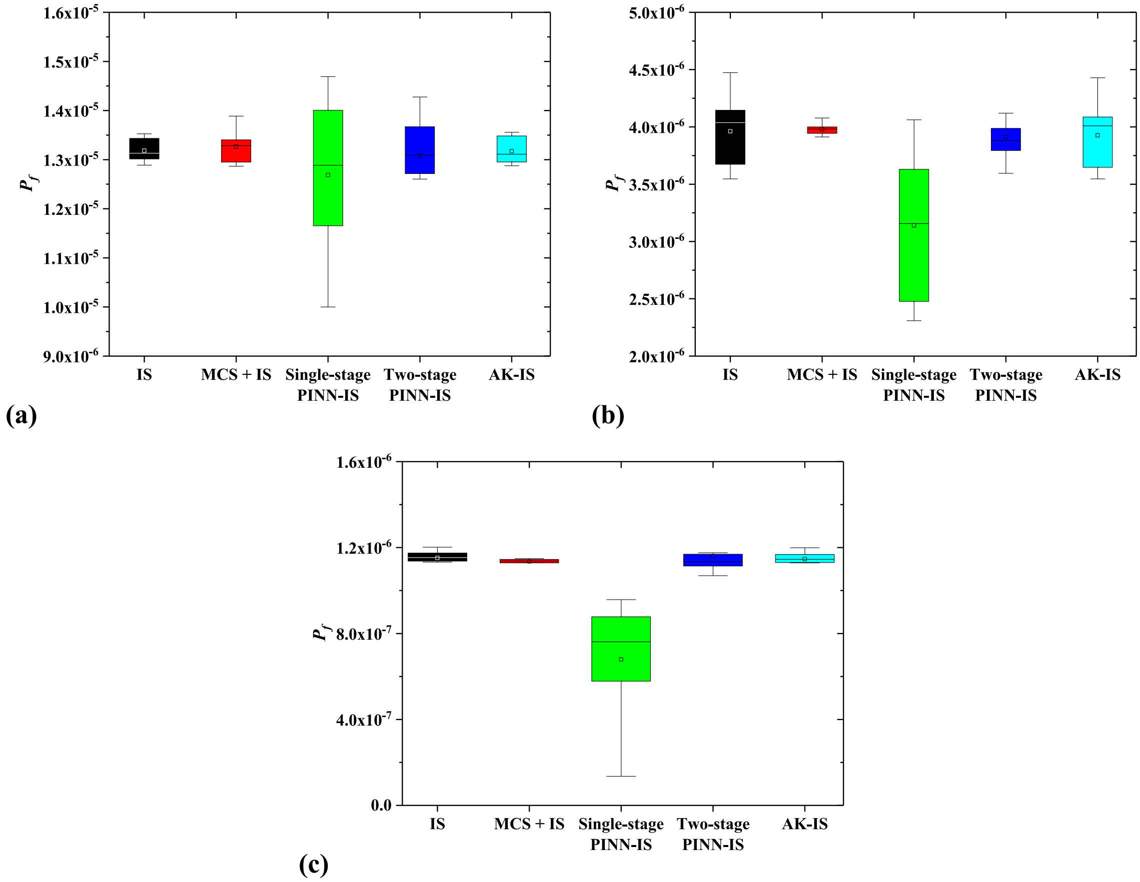

Fig. 7. Summary of statistical observation on results obtained from repetitions of different reliability analysis approaches for (a) $u_{max} = 0.2$ m, (b) $u_{max} = 0.21$ m and (c) $u_{max} = 0.22$ m.

Table 7
Results of reliability analysis for the thin square plate.

Reliability approach	P_f, [no. of function evaluations] and (absolute error in %)		
	$u_{max} = 0.2$ m	$u_{max} = 0.21$ m	$u_{max} = 0.22$ m
FORM	2.317×10^{-4} [37]	5.124×10^{-4} [37]	2.112×10^{-5} [37]
IS	1.318×10^{-5} [37 + 50,000]	3.962×10^{-6} [37 + 50,000]	1.152×10^{-6} [37 + 50,000]
AK-IS	1.317×10^{-5} [37 + 0]	3.927×10^{-6} [37 + 0]	1.146×10^{-6} [37 + 0]
MCS + IS	1.326×10^{-5} [10^6 + 50,000]	3.981×10^{-6} [10^6 + 50,000]	1.136×10^{-6} [10^6 + 50,000]
Single-stage PINN-IS	1.269×10^{-5} [nil] (4.33%)	3.141×10^{-6} [nil] (21.10%)	6.795×10^{-7} [nil] (40.16%)
Two-stage PINN-IS	1.308×10^{-5} [nil] (1.36%)	3.913×10^{-6} [nil] (1.70%)	1.159×10^{-6} [nil] (2.10%)

interests or personal relationships that could have appeared to influence the work reported in this paper.

Data availability

Data will be made available on request.

References

[1] A. Der Kiureghian, O. Ditlevsen, Aleatory or epistemic? Does it matter? Struct. Saf. 31 (2009) 105–112, https://doi.org/10.1016/j.strusafe.2008.06.020.
[2] A. Haldar, S. Mahadevan, Probability, Reliability, and Statistical Methods in Engineering Design, John Wiley, 2000.
[3] O. Ditlevsen, H.O. Madsen, Structural Reliability Methods, Wiley, 2005.
[4] Kiureghian A. Der, Structural reliability methods for seismic safety assessment: a review, Eng. Struct. 18 (1996) 412–424, https://doi.org/10.1016/0141-0296(95)00005-4.
[5] A. Der Kiureghian, Structural and System Reliability, Cambridge University Press, 2022, https://doi.org/10.1017/9781108991889.
[6] R. Rackwitz, Structural Reliability — Analysis and Prediction, vol. 23, 2001, https://doi.org/10.1016/s0167-4730(01)00007-8.
[7] R. Rackwitz, B. Fiessler, Structural reliability under combined random load sequences, Comput. Struct. 9 (1978) 489–494, https://doi.org/10.1016/0045-7949(78)90046-9.
[8] B. Keshtegar, Z. Meng, A hybrid relaxed first-order reliability method for efficient structural reliability analysis, Struct. Saf. 66 (2017) 84–93, https://doi.org/10.1016/j.strusafe.2017.02.005.
[9] A. Der Kiureghian, M De Stefano, Efficient algorithm for second-order reliability analysis, J. Eng. Mech. 117 (1991) 2904–2923, https://doi.org/10.1061/(asce)0733-9399(1991)117:12(2904.
[10] Kiureghian A. Der, H. Lin, S. Hwang, SecondOrder reliability approximations, J. Eng. Mech. 113 (1987) 1208–1225, https://doi.org/10.1061/(ASCE)0733-9399(1987)113:8(1208.
[11] A. Der Kiureghian, T. Dakessian, Multiple design points in first and second-order reliability, Struct. Saf. 20 (1998) 37–49, https://doi.org/10.1016/S0167-4730(97)00026-X.
[12] M. Shinozuka, Basic analysis of structural safety, J. Struct. Eng. 109 (1983) 721–740, https://doi.org/10.1061/(ASCE)0733-9445(1983)109:3(721.
[13] S. Engelund, R. Rackwitz, A benchmark study on importance sampling techniques in structural reliability, Struct. Saf. 12 (1993) 255–276, https://doi.org/10.1016/0167-4730(93)90056-7.
[14] Y. Ibrahim, Observations on applications of importance sampling in structural reliability analysis, Struct. Saf. 9 (1991) 269–281, https://doi.org/10.1016/0167-4730(91)90049-F.
[15] R.E. Melchers, Radial importance sampling for structural reliability, J. Eng. Mech. 116 (1990) 189–203, https://doi.org/10.1061/(ASCE)0733-9399(1990)116:1(189.
[16] S.-K. Au, J.L. Beck, Estimation of small failure probabilities in high dimensions by subset simulation, Probabilist. Eng. Mech. 16 (2001) 263–277, https://doi.org/10.1016/S0266-8920(01)00019-4.

[17] S.K. Au, J. Ching, J.L. Beck, Application of subset simulation methods to reliability benchmark problems, Struct. Saf. 29 (2007) 183–193, https://doi.org/10.1016/J.STRUSAFE.2006.07.008.

[18] H.J. Pradlwarter, G.I. Schuëller, P.S. Koutsourelakis, D.C. Charmpis, Application of line sampling simulation method to reliability benchmark problems, Struct. Saf. 29 (2007) 208–221, https://doi.org/10.1016/J.STRUSAFE.2006.07.009.

[19] Z. Lu, S. Song, Z. Yue, J. Wang, Reliability sensitivity method by line sampling, Struct. Saf. 30 (2008) 517–532, https://doi.org/10.1016/J.STRUSAFE.2007.10.001.

[20] O. Ditlevsen, R.E. Melchers, H. Gluver, General multi-dimensional probability integration by directional simulation, Comput. Struct. 36 (1990) 355–368, https://doi.org/10.1016/0045-7949(90)90134-N.

[21] L. Faravelli, Response-surface approach for reliability analysis, J. Eng. Mech. 115 (1989) 2763–2781, https://doi.org/10.1061/(ASCE)0733-9399(1989)115:12(2763.

[22] C. Kim, S. Wang, K.K. Choi, Efficient response surface modeling by using moving least-squares method and sensitivity, AIAA J. 43 (2005) 2404–2411, https://doi.org/10.2514/1.12366.

[23] I. Kaymaz, Application of kriging method to structural reliability problems, Struct. Saf. 27 (2005) 133–151.

[24] G. Li, T. Wang, Z. Chen, J. He, X. Wang, X. Du, RBIK-SS: a parallel adaptive structural reliability analysis method for rare failure events, Reliab. Eng. Syst. Saf. 239 (2023) 109513, https://doi.org/10.1016/J.RESS.2023.109513.

[25] Elhewy A. Hosni, E. Mesbahi, Y. Pu, Reliability analysis of structures using neural network method, Probabilist. Eng. Mech. 21 (2006) 44–53, https://doi.org/10.1016/J.PROBENGMECH.2005.07.002.

[26] J.P.S. Lima, F. Evangelista, C. Guedes Soares, Hyperparameter-optimized multi-fidelity deep neural network model associated with subset simulation for structural reliability analysis, Reliab. Eng. Syst. Saf. 239 (2023) 109492, https://doi.org/10.1016/J.RESS.2023.109492.

[27] J. Deng, Structural reliability analysis for implicit performance function using radial basis function network, Int. J. Solid Struct. 43 (2006) 3255–3291, https://doi.org/10.1016/J.IJSOLSTR.2005.05.055.

[28] A. Roy, R. Manna, S. Chakraborty, Support vector regression based metamodeling for structural reliability analysis, Probabilist. Eng. Mech. 55 (2019) 78–89, https://doi.org/10.1016/j.probengmech.2018.11.001.

[29] A. Roy, S. Chakraborty, Reliability analysis of structures by a three-stage sequential sampling based adaptive support vector regression model, Reliab. Eng. Syst. Saf. 219 (2022) 108260, https://doi.org/10.1016/j.ress.2021.108260.

[30] A. Roy, S. Chakraborty, Support vector machine in structural reliability analysis: a review, Reliab. Eng. Syst. Saf. 233 (2023) 109126, https://doi.org/10.1016/j.ress.2023.109126.

[31] A. Roy, S. Chakraborty, S. Adhikari, Reliability analysis of structures by active learning enhanced sparse bayesian regression, J. Eng. Mech. 149 (2023) 04023024, https://doi.org/10.1061/jenmdt.emeng-6964.

[32] M. Dong, Y. Cheng, L. Wan, A new adaptive multi-kernel relevance vector regression for structural reliability analysis, Reliab. Eng. Syst. Saf. 243 (2024) 109890, https://doi.org/10.1016/J.RESS.2023.109890.

[33] B. Sudret, A. Der Kiureghian, Comparison of finite element reliability methods, Probabilist. Eng. Mech. 17 (2002) 337–348, https://doi.org/10.1016/S0266-8920(02)00031-0.

[34] P.T.T. Nguyen, L. Manuel, Uncertainty quantification in low-probability response estimation using sliced inverse regression and polynomial chaos expansion, Reliab. Eng. Syst. Saf. 242 (2024) 109750, https://doi.org/10.1016/J.RESS.2023.109750.

[35] M. Raissi, P. Perdikaris, G.E. Karniadakis, Physics-informed neural networks: a deep learning framework for solving forward and inverse problems involving nonlinear partial differential equations, J. Comput. Phys. 378 (2019) 686–707, https://doi.org/10.1016/j.jcp.2018.10.045.

[36] A.G. Baydin, B.A. Pearlmutter, A.A. Radul, J.M. Siskind, Automatic differentiation in machine learning: a survey, J. Mach. Learn. Res. 18 (2018) 1–43.

[37] Y. Yang, P. Perdikaris, Adversarial uncertainty quantification in physics-informed neural networks, J. Comput. Phys. 394 (2019) 136–152, https://doi.org/10.1016/J.JCP.2019.05.027.

[38] L. Yang, X. Meng, G.E. Karniadakis, B-PINNs: Bayesian physics-informed neural networks for forward and inverse PDE problems with noisy data, J. Comput. Phys. 425 (2021) 109913, https://doi.org/10.1016/J.JCP.2020.109913.

[39] S. Wang, X. Yu, P. Perdikaris, When and why PINNs fail to train: a neural tangent kernel perspective, J. Comput. Phys. 449 (2022) 110768, https://doi.org/10.1016/j.jcp.2021.110768.

[40] T. Chatterjee, M.I. Friswell, S. Adhikari, H.H. Khodaparast, MATLAB implementation of physics informed deep neural networks for forward and inverse structural vibration problems, Aerosp Res Commun 2 (2024) 13194, https://doi.org/10.3389/ARC.2024.13194.

[41] S. Chakraborty, Transfer learning based multi-fidelity physics informed deep neural network, J. Comput. Phys. 426 (2021) 109942, https://doi.org/10.1016/J.JCP.2020.109942.

[42] X. Meng, G.E. Karniadakis, A composite neural network that learns from multi-fidelity data: application to function approximation and inverse PDE problems, J. Comput. Phys. 401 (2020) 109020, https://doi.org/10.1016/J.JCP.2019.109020.

[43] S. Garg, S. Chakraborty, B. Hazra, Physics-integrated hybrid framework for model form error identification in nonlinear dynamical systems, Mech. Syst. Signal Process. 173 (2022) 109039, https://doi.org/10.1016/J.YMSSP.2022.109039.

[44] G.E. Karniadakis, I.G. Kevrekidis, L. Lu, P. Perdikaris, S. Wang, L. Yang, Physics-informed machine learning, Nat Rev Phys 3 (2021) 422–440, https://doi.org/10.1038/s42254-021-00314-5.

[45] T. Chatterjee, M.I. Friswell, S. Adhikari, H.H. Khodaparast, Gradient enhanced physics-informed neural networks for digital twins of structural vibrations, in: M. C. Leva, E. Patelli, L. Podofillini, S. Wilson (Eds.), Proc. 32nd Eur. Saf. Reliab. Conf., Research Publishing, Singapore, 2023, pp. 2586–2593, https://doi.org/10.3850/978-981-18-5183-4_s14-09-554-cd.

[46] T. Liu, H. Meidani, Physics-informed neural networks for system identification of structural systems with a multiphysics damping model, J. Eng. Mech. 149 (2023) 04023079, https://doi.org/10.1061/JENMDT.EMENG-7060/ASSET/226EE73A-53D1-4152-B68A-5576EE2EEEFF/ASSETS/IMAGES/LARGE/FIGURE11.JPG.

[47] J.H. Bastek, D.M. Kochmann, Physics-informed neural networks for shell structures, Eur. J. Mech. Solid. 97 (2023) 104849, https://doi.org/10.1016/J.EUROMECHSOL.2022.104849.

[48] M.A. Roehrl, T.A. Runkler, V. Brandtstetter, M. Tokic, S. Obermayer, Modeling system dynamics with physics-informed neural networks based on Lagrangian mechanics, IFAC-PapersOnLine 53 (2020) 9195–9200, https://doi.org/10.1016/J.IFACOL.2020.12.2182.

[49] Y. Yu, H. Yao, Y. Liu, Structural dynamics simulation using a novel physics-guided machine learning method, Eng. Appl. Artif. Intell. 96 (2020) 103947, https://doi.org/10.1016/j.engappai.2020.103947.

[50] U. Tripathi, S. Garg, R. Nayek, S. Chakraborty, Physics-integrated deep learning for uncertainty quantification and reliability estimation of nonlinear dynamical systems, Probabilist. Eng. Mech. 72 (2023) 103419, https://doi.org/10.1016/J.PROBENGMECH.2023.103419.

[51] Y. Xu, S. Kohtz, J. Boakye, P. Gardoni, P. Wang, Physics-informed machine learning for reliability and systems safety applications: state of the art and challenges, Reliab. Eng. Syst. Saf. 230 (2023), https://doi.org/10.1016/J.RESS.2022.108900.

[52] S. Chakraborty, Simulation free reliability analysis: a physics-informed deep learning based approach, Jun 2020, Accessed: 13 October 2024. [Online]. Available: https://arxiv.org/abs/2005.01302v3.

[53] R. Teixeira, M. Nogal, A. O'Connor, Adaptive approaches in metamodel-based reliability analysis: a review, Struct. Saf. 89 (2021) 102019, https://doi.org/10.1016/j.strusafe.2020.102019.

[54] C. Zhang, A. Shafieezadeh, Simulation-free reliability analysis with active learning and Physics-Informed Neural Network, Reliab. Eng. Syst. Saf. 226 (2022) 108716, https://doi.org/10.1016/j.ress.2022.108716.

[55] Z. Meng, Q. Qian, M. Xu, B. Yu, A.R. Yıldız, S. Mirjalili, PINN-FORM: a new physics-informed neural network for reliability analysis with partial differential equation, Comput. Methods Appl. Mech. Eng. 414 (2023) 116172, https://doi.org/10.1016/J.CMA.2023.116172.

[56] T. Zhou, X. Zhang, E.L. Droguett, A. Mosleh, A generic physics-informed neural network-based framework for reliability assessment of multi-state systems, Reliab. Eng. Syst. Saf. 229 (2023) 108835, https://doi.org/10.1016/J.RESS.2022.108835.

[57] T. Zhou, E.L. Droguett, A. Mosleh, Physics-informed deep learning: a promising technique for system reliability assessment, Appl. Soft Comput. 126 (2022) 109217, https://doi.org/10.1016/J.ASOC.2022.109217.

[58] Z. Bai, S. Song, Physics-informed neural network for first-passage reliability assessment of structural dynamic systems, Comput. Struct. 289 (2023) 107189, https://doi.org/10.1016/J.COMPSTRUC.2023.107189.

[59] S. Das, S. Tesfamariam, Reliability assessment of stochastic dynamical systems using physics informed neural network based PDEM, Reliab. Eng. Syst. Saf. 243 (2024) 109849, https://doi.org/10.1016/J.RESS.2023.109849.

[60] I. Lee, U. Lee, P. Ramu, D. Yadav, G. Bayrak, E. Acar, Small failure probability: principles, progress and perspectives, Struct. Multidiscip. Optim. 65 (2022) 1–34, https://doi.org/10.1007/S00158-022-03431-6/TABLES/9.

[61] F. Cadini, F. Santos, E. Zio, An improved adaptive kriging-based importance technique for sampling multiple failure regions of low probability, Reliab. Eng. Syst. Saf. 131 (2014) 109–117, https://doi.org/10.1016/J.RESS.2014.06.023.

[62] J. Zhou, J. Li, An enhanced method for improving the accuracy of small failure probability of structures, Reliab. Eng. Syst. Saf. 228 (2022) 108784, https://doi.org/10.1016/J.RESS.2022.108784.

[63] J.M. Bourinet, Rare-event probability estimation with adaptive support vector regression surrogates, Reliab. Eng. Syst. Saf. 150 (2016) 210–221, https://doi.org/10.1016/j.ress.2016.01.023.

[64] X. Zhang, L. Wang, J.D. Sørensen, REIF: a novel active-learning function toward adaptive Kriging surrogate models for structural reliability analysis, Reliab. Eng. Syst. Saf. 185 (2019) 440–454, https://doi.org/10.1016/j.ress.2019.01.014.

[65] C. Xu, W. Chen, J. Ma, Y. Shi, S. Lu, AK-MSS: an adaptation of the AK-MCS method for small failure probabilities, Struct. Saf. 86 (2020) 101971, https://doi.org/10.1016/j.strusafe.2020.101971.

[66] B. Echard, N. Gayton, M. Lemaire, N. Relun, A combined Importance Sampling and Kriging reliability method for small failure probabilities with time-demanding numerical models, Reliab. Eng. Syst. Saf. 111 (2013) 232–240, https://doi.org/10.1016/j.ress.2012.10.008.

[67] W. Li, R. Geng, S. Chen, CSP-free adaptive Kriging surrogate model method for reliability analysis with small failure probability, Reliab. Eng. Syst. Saf. (2023) 109898, https://doi.org/10.1016/J.RESS.2023.109898.

[68] A. Dasgupta, E.A. Johnson, REIN: reliability estimation via importance sampling with normalizing flows, Reliab. Eng. Syst. Saf. 242 (2024) 109729, https://doi.org/10.1016/J.RESS.2023.109729.

[69] M.A. Nabian, R.J. Gladstone, H. Meidani, Efficient training of physics-informed neural networks via importance sampling, Comput Civ Infrastruct Eng 36 (2021) 962–977, https://doi.org/10.1111/MICE.12685.

[70] A. Harbitz, Efficient and accurate probability of failure calculation by the use of importance sampling technique, Int. Conf. Appl. Stat. Probab. Soil Struct. Eng. 4 (1983) 825–886.
[71] R.E. Melchers, Importance sampling in structural systems, Struct. Saf. 6 (1989) 3–10, https://doi.org/10.1016/0167-4730(89)90003-9.
[72] S. Au, Y. Wang, Engineering Risk Assessment with Subset Simulation, vol. 9781118398043, Wiley, 2014, https://doi.org/10.1002/9781118398050.